

Directional acoustic source by scattering acoustical elements

Andreas Håkansson^{a)}

International Center for Young Scientists, National Institute for Materials Science (NIMS), 1-1 Namiki, Tsukuba 305-0044, Japan

Daniel Torrent, Francisco Cervera, and José Sánchez-Dehesa^{b)}

Wave Phenomena Group, Department of Electronic Engineering, Polytechnic University of Valencia, C/Camino de Vera s.n., E-46022 Valencia, Spain

(Received 20 December 2006; accepted 5 May 2007; published online 1 June 2007)

Highly directional sources are desirable in a variety of fields for many applications. The authors report an inverse designed scattering acoustical element device that transforms an omnidirectional ultrasonic source into one highly directional. This two-dimensional design shows an overall better modeled performance than other previously proposed, including a half-power angular width less than 5° . The experimental demonstration is performed in the ultrasonic range, using a hydrophone as omnidirectional source and an array of alumina rods as building blocks for the scattering acoustical elements. The measured half-power angular width is 6° , a value that supports the high reliability of the designing tool. © 2007 American Institute of Physics. [DOI: 10.1063/1.2743947]

Phononic crystals (PCs) are manufactured materials consisting of periodic distributions of two (or more) materials with different elastic properties. Recent research on PC demonstrates their prospects as efficient materials in controlling the propagation of sound in a similar way as photonic crystals do for electromagnetic waves. For example, since the demonstration of the phononic band gaps, PCs have been proposed as filter devices and sound shields.¹ Furthermore, their extraordinary refractive properties have been used to focus waves by exercising either the positive refraction² or the negative refraction.^{3,4}

More recently, directional acoustic sources (DASs) based on two-dimensional (2D) PC were proposed by using two different approaches. The first proposal⁵ uses the phononic band gap to design a cavity. To achieve collimation a line source is placed inside the planar cavity which then radiates collimated sound at the resonant frequency. The second proposal⁶ consists of tuning the frequency of the source so that it coincide to the band edge K_2 of the embedded 2D PC. The strong coupling with the band-edge states will make the PC suitable as a DAS device. Unfortunately, no experimental demonstration has been presented to date of any of them and, therefore, we have no knowledge about the efficiency of the underlying coupling mechanism assumed in such proposals.

In parallel with the study of PC, optimization or inverse design (ID) of phononic devices is rapidly developing. One goal of this line of research is to bring functionalities, similar to those proposed by periodic structures, to perfection without demanding any ordering of the scattering units. Recently, a family of acoustical devices based on ID was introduced named scattering acoustical elements (SAEs). A SAE consists of a few layers of cylindrical scatterers whose shape and positions are ID to accomplish a given functionality. Various SAEs with innovative functionalities have been proposed and experimentally demonstrated to date, e.g., flat acoustic lenses⁷ and demultiplexing devices.⁸

In this letter a SAE-DAS device is presented and characterized. The calculated properties show optimized control of the sound directionality emitted from an omnidirectional point source, including enhancement at the emitted wavelength, and directionality of the scattered sound emitted by the source. Furthermore, the measured performance of the prototype (see Fig. 1) confirms the quality of the design approach and the modeling tools.

The ID tool employed in the design of the SAE-DAS is an integration of a direct solver, the multiple scattering theory, and a global optimization method, the genetic algorithm. For technical details of the ID procedure the reader is addressed to Ref. 9 and references therein. To narrow down the search space of the ID process we employ a set of constraints, set according to the limitations of the prototype fabrication process. The first constraint is related to the scattering objects, which consist of straight cylinders with circular section perfectly aligned. More specifically, 40 cm long rods of alumina with a density of 3860 kg/m^3 , placed in water, are used in the prototype fabrication. The huge contrast between acoustic impedances Z between cylinders and water ($Z_{\text{cyl}} > 100Z_w$) justifies the simplifying assumption of rigid cylinders ($\rho_{\text{cyl}} = \infty$); i.e., no sound excitation inside cylinders. The position and diameter of the rods can be chosen almost freely; however, for simplicity we will use circular shaped rods of diameter of 0.6 cm and positions constrained to a

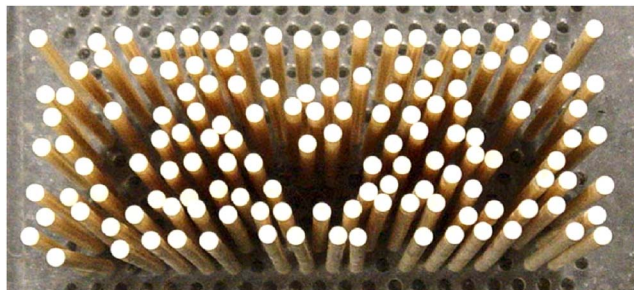


FIG. 1. (Color online) Photograph (taken from the top) of the scattering acoustical element designed to get a highly directional acoustic source. The hydrophone is put at the central cavity.

^{a)}Electronic mail: hakansson.andreas@nims.go.jp

^{b)}Electronic mail: jsdehesa@upvnet.upv.es

hexagonal lattice array with lattice parameter of 1.05 cm. However, even under these constraints the ID method gives a great number of different possible designs to work with. This large variation is an important part of the design process.

The goal is to find a SAE-DAS device that highly collimates the emitted wavelength by the source that is assumed to be placed at the center of the device $(x_0, y_0) = (0.0, 0.0)$. In other words, the objective of the ID process is to design a device that will transform an embedded omnidirectional source into a highly collimated one. Hence, in the design process a point source is employed as the emitting source with a 2D field distribution as $H_0^{(1)}(kr)e^{-i\phi}$, where $H_0^{(1)}$ is the Hankel function of first kind and zero order and k is the wave vector. The source is embedded inside nine layers, i.e., five layers in the backward direction and three in the forward. The odd distribution of layers is set to minimize the backward scattering. Though an increase in layers would likely result in a better performance, the number of layers is intentionally kept low to facilitate the fabrication process.

The inverse problem is set up to find a device with a maximum value of the pressure modulus $|P(x, y)|$ at a far field point in the forward direction for the wavelength $\lambda_0 = 1.125$ cm. This point is taken at a distance $r_0 = 100$ cm from the source on the x axis. Figure 2 shows the cross section of the maximized device as well as its predicted performance. The square of the pressure modulus is represented in the near field [Fig. 2(a)] and in the far field [Fig. 2(b)]. Also, the radiation pattern around the SAE-DAS is depicted at two distances from the device, in Fig. 2(c), i.e., at the measurement radius ($r_0 = 25$ cm) and at the radius employed by the optimization procedure ($r_0 = 100$ cm). We have estimated the radiation efficiency of the acoustical source by calculating the parameters characterizing this kind of devices.^{5,6} The far field normalized energy-flux density (NEFD) was calculated at the optimal wavelength of λ_0 . We integrate the NEFD over all directions in the far field. The total energy radiated along all the directions, γ , is a good estimation of the radiation behavior of the SAE-DAS.⁵ The calculated γ is about 31 times of that for free radiation. The radiation of the two narrow angular regions [$\theta = 0^\circ$ and $\theta = 180^\circ$, respectively, in Fig. 2(c)] comprises about 76.6% of the whole radiating energy, with 67.3% along the $+x$ direction [$\theta = 0^\circ$ in Fig. 2(c)]. The half-power angular width (HPAW) for the forward peak is 4.6° . A comparison with previous DAS also theoretically proposed is shown in Table I. It is noticeable how the ID SAE-DOS outperforms in overall performance the others based on PC. Also, it must be stressed that the extraordinary performance of our ID device is achieved with a minimum number of cylinders.

To characterize the SAE-DAS a prototype of the designed device was constructed by fixing alumina cylinder in a metacrylate plate with drilled holes (see Fig. 1). The arrangement of the cylinders surrounding the hydrophone, which is embedded at the center, is clearly seen in the top view. The characterization of the SAE-DAS was performed in a water tank by using an experimental setup that consists of two hydrophones, a signal generator and a data acquisition system. We use high sensitive hydrophones of 1 cm of diameter size that are omnidirectional for high frequencies and have a usable frequency range of 100 kHz–170 kHz. The source hydrophone is put at the equatorial plane of the structure and defines the origin of the coordinate system. The second hydrophone acts as receiver and it is attached to a

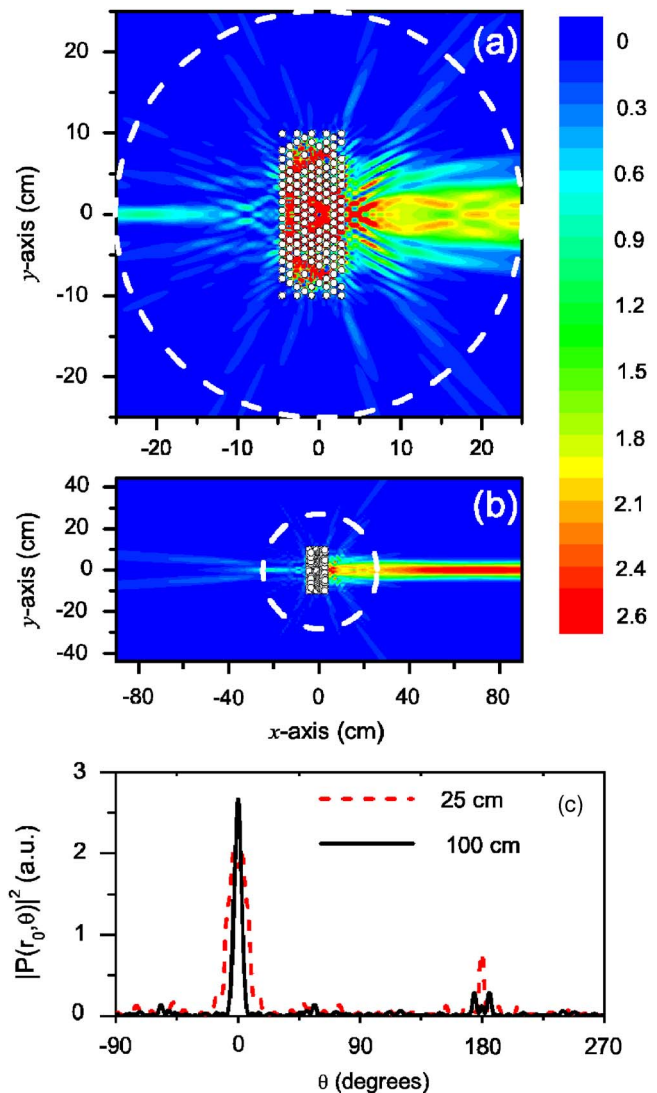


FIG. 2. (Color online) Performance of the optimized SAE-DAS device at the central wavelength of the emitting source. (a) Square of the sound pressure in the near field. (b) Square of the pressure showing the collimation of sound emission in the far field. The white circles define the position of solid rods in the SAE-DAS device. The white dashed circumferences represent the positions scanned by the experimental setup. (c) Angular dependence at two distances from the center of the device.

robotic arm that scans the sound around a circular path of radius $r_0 = 25$ cm. This distance was determined by the dimension of our tank. The source emits a Gaussian pulse with frequencies in the range from 115 up to 135 kHz, enclosing the frequency employed in the optimization procedure. A total of ten spectra have been taken to generate the average spectrum finally assigned to each θ . Figure 3 shows the square of the pressure map $|P(r_0, \theta)|^2$ obtained with a reso-

TABLE I. Radiation properties of proposed SAE-DAS compared with other theoretical proposals, including the number of cylinders employed in its design (N), total radiation enhancement factor (γ), half power angular width (HPAW), and relevant radiation efficiency in the principal direction of emission (η_{+x}).

| | N | γ | HPAW | $\eta_{+x}(\%)$ |
|---------|-----|----------|-------------|-----------------|
| SAE-DAS | 136 | 31 | 4.6° | 67.3 |
| Ref. 6 | 384 | 8.7 | 5.2° | 72.3 |
| Ref. 5 | 220 | 7.4 | 5.8° | 65.5 |

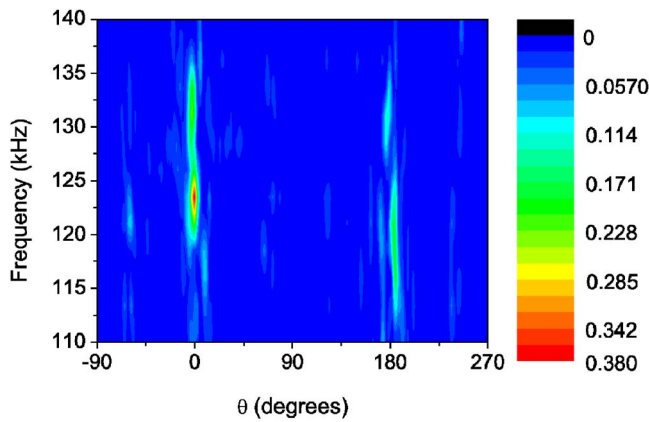


FIG. 3. (Color online) Measured sound emission modification by the inverse designed SAE-DAS of an omnidirectional hydrophone emitting in the range from 115 up to 135 kHz.

lution of 2.5 kHz in frequency and 1° in θ . It is noticeable how the emitted radiation is highly collimated along the forward direction ($+x$), though some energy is also emitted along the backwards direction ($-x$), as was theoretically predicted. Figure 4 depicts the measured angular dependence for 123.5 kHz, which corresponds to the maximum intensity peak in Fig. 3. This frequency is slightly smaller than that employed in the ID procedure. The measured radiation of the two narrow angular regions in Fig. 4 comprises about 46.7% of the whole radiating energy, with 45.7% along the forward direction and only 1.0% along the backward direction. The measured HPAW is 6° , which is slightly larger than that predicted at the far field (see Table I) but is lower than that calculated at the distance of measurement, i.e., $\text{HPAW}(r_0 = 25 \text{ cm}) = 17.6^\circ$ [see Fig. 2(c)]. The discrepancy between

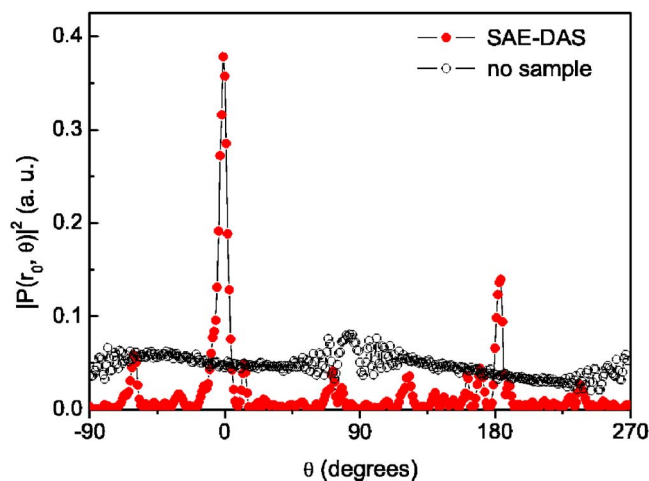


FIG. 4. (Color online) Measured angular dependence at a radius of 25 cm from the center of the device. The black symbols report the data corresponding when no sample is in the setup.

calculated and measured HPAWs probably comes from the fact that the frequencies (theoretical and experimental) at which the phenomenon is observed are slightly different.

In conclusion, it has been demonstrated that by using inverse design one can achieve high control of the emission pattern of sound sources. Furthermore, the design process is carried out under the limitations of the materials we have at hands. In particular, it has been shown how the emitted sound by a hydrophone can be controlled in the plane by surrounding it with an array of scatterers and so controlling the directionality of sound emission. We believe that this demonstration is an important step in various fields of acoustics. Also, since the ID method could be improved along with fabrication method, many constraints could be removed and we will have more freedom of design that will result in an increase of the asked for performance of the optimal design.

This study was performed through Special Coordination Fund for Promoting Science and Technology from the MEXT, Japan. Work partially financed by the Spanish MEC (Contract No. TEC2004-02345). One of the authors (J.S.-D.) acknowledges the support of K. Sakoda and H. T. Miyazaki, and the facilities provided by the Nanophotonics Group during his visit at NIMS. Daniel Torrent acknowledges a PhD grant paid by MEC.

Note added during proofs. The authors found two articles that are relevant to the work reported here. The first one by Ke and coworkers¹⁰ presents an experimental demonstration of the proposal introduced in Ref. 5. Their reported data show a radiation field with half-power beam width of less than 6° . The second one by Wu and coworkers¹¹ reports a design of a highly directional acoustic source based on the planar resonant cavity of two-dimensional phononic crystal.

¹J. V. Sánchez-Perez, D. Caballero, R. Martínez-Sala, C. Rubio, J. Sánchez-Dehesa, F. Meseguer, J. Llinares, and F. Galvez, *Phys. Rev. Lett.* **80**, 5325 (1998).

²F. Cervera, L. Sanchis, J. V. Sánchez-Perez, R. Martínez-Sala, C. Rubio, F. Meseguer, C. Lopez, D. Caballero, and J. Sánchez-Dehesa, *Phys. Rev. Lett.* **88**, 023902 (2002).

³X. Hu, Y. Shen, X. Li, R. Liu, R. Fu, and J. Zi, *Phys. Rev. E* **69**, 030201 (2004).

⁴X. Zhang and Z. Liu, *Appl. Phys. Lett.* **85**, 341 (2004).

⁵C. Qiu, Z. Liu, J. Shi, and C. T. Chan, *Appl. Phys. Lett.* **86**, 224105 (2005).

⁶C. Qiu and Z. Liu, *Appl. Phys. Lett.* **89**, 063106 (2006).

⁷A. Håkansson, F. Cervera, and J. Sánchez-Dehesa, *Appl. Phys. Lett.* **86**, 054102 (2005).

⁸A. Håkansson, J. Sánchez-Dehesa, and F. Cervera, *Appl. Phys. Lett.* **88**, 163506 (2006).

⁹A. Håkansson, J. Sánchez-Dehesa, and L. Sanchis, *Phys. Rev. B* **70**, 214302 (2004).

¹⁰M. Ke, Z. Liu, P. Pang, W. Wabg, Z. Cheng, J. Shi, X. Zhao, W. Wen, *Appl. Phys. Lett.* **88**, 263505 (2006).

¹¹T.-T. Wu, C. H. Hsu, and J. H. Sun, *Appl. Phys. Lett.* **89**, 171912 (2006).